THE JOURNAL OF PHYSICAL CHEMISTRY C

Article

Cite This: J. Phys. Chem. C XXXX, XXX, XXX−XXX

pubs.acs.org/JPCC

Precise Tailoring of Ir-FeO_x Interfaces for Improved Catalytic Performance in Preferential Oxidation of Carbon Monoxide in Hydrogen

Chunlei Wang, Qi Yao, Lina Cao, Junjie Li, Si Chen, and Junling Lu*

Department of Chemical Physics, Hefei National Laboratory for Physical Sciences at the Microscale, Key Laboratory of Surface and Interface Chemistry and Energy Catalysis of Anhui Higher Education Institutes, iChEM, CAS Key Laboratory of Materials for Energy Conversion, University of Science and Technology of China, Hefei, Anhui 230026, P. R. China

ABSTRACT: Preferential oxidation of CO in H_2 (PROX) has been regarded as the most promising on-board approach to remove the trace levels of CO (~1%) present in hydrogen fuels and thus to protect the Pt electrodes of proton exchange membrane fuel cells (PEMFCs) against CO poisoning. However, development of an active and selective catalyst toward CO oxidation in a broad low-temperature range remains challenging due to the competitive hydrogen oxidation reaction. Here, we report that selective deposition of the FeO_x overcoat onto SiO_2-supported Ir nanoparticles using the atomic layer deposition (ALD) technique allows precisely tailoring Ir−FeO_x interfaces for optimizing catalytic performance in the PROX reaction. Compared to the uncoated Ir/SiO_2 sample, FeO_x-coated Ir/SiO_2 samples exhibited remarkable activity enhancements, where we observed a volcano trend of the improved activity as a function of the numbers of FeO_x ALD cycles. The optimized catalytic performance was achieved on a 1.5 nm Ir/SiO_2 sample with two cycles of FeO_x overcoating, by achieving complete CO conversion in a broad temperature range of 60−180 °C in the PROX reaction, which is the broadest temperature range over Ir-based catalysts reported in the literature so far. We noticed that the activity improvement over these samples was much less pronounced in CO oxidation in the absence of H_2, which implies that the formation of hydroxyls on the FeO_x overcoat might be attributed to the large activity enhancement in the PROX reaction.

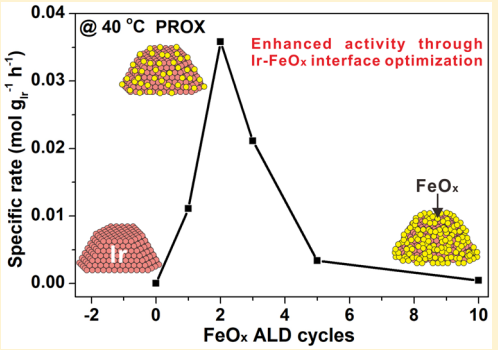

1. INTRODUCTION

Proton-exchange membrane fuel cells (PEMFCs) are considered to be one of the most attractive technologies for efficient and environmentally benign power generations in the applications of transportation, residential cogeneration, portable electric devices, and others.[1,2] One obstacle is that the hydrogen fuel, generally produced by reforming of hydrocarbons or alcohols, often contains ~1% CO impurities,[3] which can deactivate the platinum electrodes quickly.[4] Preferential CO oxidation in H_2 (PROX) is the promising on-board approach to remove the CO residuals for protecting the fuel cells against CO poisoning.[5−7] The goal is to develop a catalyst active and selective toward CO oxidation in rich H_2 over a broad low-temperature range, so that CO can be efficiently removed (below 10 ppm) on board during PEMFC operation.[1,8] However, the competitive H_2 oxidation reaction makes the above demand challenging.

In the past decades, tremendous efforts have been devoted to developing an efficient PROX catalyst by examining a broad scope of catalyst candidates including CuO_x−CeO_x,[9,10] Au,[11−13] and Pt-group catalysts.[14−16] Among these catalysts investigated, Pt-group catalysts with a promotion of transition metal oxide (TMO_x), e.g., FeO_x, showed remarkably high catalytic performance in both activity and selectivity toward CO oxidation. For instance, Zhang et al. showed that subnanometer Pt clusters supported on iron oxide enabled us to achieve complete CO conversion in a low-temperature range of 20−70 °C in the PROX reaction.[17] Watanabe et al. reported that zeolite-supported PtFe alloy nanoparticles (NPs) with a particle size of ~1.1 nm could achieve complete CO conversion in a higher broad temperature range of 80−200 °C.[18] Bao et al. proposed that the largely improved activity over PtFe/SiO_2 in the PROX reaction stems from the confined CO oxidation reaction at the Pt−FeO interfaces through the noncompetitive Langmuir−Hinshelwood mechanism where CO chemisorbs on the Pt surface and O_2 is activated at the interface.[19] Contacting FeO_x (or $Fe(OH)_x$) with Ir NPs also illustrated similar activity promotions by achieving complete CO conversion in a low-temperature range of 20−60 °C.[20,21] Therefore, effective construction of metal−oxide interfaces is a promising way to optimize the catalytic performance. However, in fact, it is difficult to realize this purpose using the conventional wet-chemistry methods due to the lack of precise control of the coverage of FeO_x on metal NPs.

Atomic layer deposition (ALD) is a thin-film growth technique, relying on sequential molecular-level self-limiting

Received: September 24, 2019
Revised: November 11, 2019
Published: November 11, 2019

DOI: 10.1021/acs.jpcc.9b09066
J. Phys. Chem. C XXXX, XXX, XXX−XXX

surface reactions. Owing to its self-limiting feature, ALD allows conformal and uniform deposition of materials with near atomic precise control on all types of substrates from two-dimensional flat materials to high-aspect-ratio materials and to high-surface-area materials.[22] Consequently, ALD has been applied in a wide range of applications, including electroluminescent displays,[23] microdevices,[24] polymers,[25] catalysts, and beyond.[26] Very recently, we reported that by utilizing the self-limiting nature of ALD and the steric hindrance between chemisorbed iron precursors FeO_x could be precisely deposited onto silica-supported Pt NPs using FeO_x ALD, where the dispersion of FeO_x species on Pt NPs could be gradually tailored by increasing the coverages. In situ spectroscopic characterization showed that iron species at low coverages were atomically dispersed $Fe_1(OH)_x$ under the PROX reaction conditions, and abundant $Pt-Fe_1(OH)_x$ single interfacial sites are formed, which boost catalytic activity tremendously by achieving complete CO removal with 100% CO selectivity over a broad low-temperature range of −75−107 °C.[27] This work suggests that ALD is a powerful tool to atomically precisely construct metal−oxide interfaces for optimized catalytic performance.

In this work, FeO_x was selectively deposited onto SiO_2-supported Ir NPs with different Ir particle sizes using ALD to precisely tailor the $Ir-FeO_x$ interfacial sites for optimizing catalytic activity in the PROX reaction. Inductively coupled plasma-atomic emission spectrometry (ICP-AES), elemental mapping, and diffuse reflectance infrared Fourier transform spectroscopy (DRIFTS) of CO chemisorption measurements confirmed the selective deposition of FeO_x on Ir NPs but not on the SiO_2 support. FeO_x-coated Ir/SiO_2 samples exhibited remarkable activity enhancements compared to the uncoated Ir/SiO_2 sample, and the improved activity showed a volcano trend with the number of FeO_x ALD cycles. Among these samples, a 1.5 nm Ir/SiO_2 sample with two cycles of FeO_x overcoat showed the optimized catalytic performance, by achieving complete CO conversion in a broad temperature range of 60−180 °C in the PROX reaction, which is the broadest temperature range over Ir-based catalysts reported in the literature so far.

2. EXPERIMENTAL SECTION

2.1. Catalyst Synthesis. *2.1.1. Ir/SiO_2 Catalyst.* Commercial SiO_2 (Sigma-Aldrich, BET surface area 300 m^2/g) was selected as the catalyst support. The Ir/SiO_2 catalyst was prepared by the incipient wetness impregnation method.[28] In brief, 1 g of $H_2IrCl_6{\cdot}xH_2O$ (Aladdin, Ir ≥ 36%) was first dissolved into 50 mL of deionized water. Next, 2.1 mL of the as-prepared H_2IrCl_6 aqueous solution and 480 mg of SiO_2 were added to 50 mL of deionized water. The mixture was stirred for 24 h at room temperature and then dried at 80 °C. The resulting material is denoted as Ir/SiO_2-UC. Next, these materials were further calcined at the different temperatures of 250, 350, and 600 °C in 10 vol % O_2 in Ar for 4 h, respectively, followed by a reduction at 300 °C in 10 vol % H_2 in Ar for another 1 h to vary the Ir particle size. These samples are denoted as Ir/SiO_2-250, Ir/SiO_2-350, and Ir/SiO_2-600, respectively.

2.1.2. Selective Deposition of FeO_x on Ir/SiO_2 Catalysts. FeO_x ALD was performed in a viscous flow reactor (GEMSTAR-6 Benchtop ALD, Arradiance) at 120 °C with a carrier gas of ultrahigh purity N_2 (99.999%) at a flow rate of 200 mL/min. Ferrocene (99.7%, Sigma-Aldrich) was used as the iron precursor, and oxygen was used as the oxidant. The ferrocene container was heated to 90 °C to achieve a reasonable vapor pressure. The reactor inlet lines were heated to 120 °C to prevent any precursor condensation. After loading an Ir/SiO_2 sample into the ALD reactor for 30 min with temperature stabilized, FeO_x ALD was performed by alternatively exposing the sample to the ferrocene vapor and oxygen for different cycles. The timing sequence was 150, 150, 100, and 150 s for the ferrocene exposure, N_2 purge, O_2 exposure, and N_2 exposure, respectively. The samples with different ALD cycles of FeO_x coating were denoted as nFe/Ir/SiO_2-X. Here n is the number of FeO_x ALD cycles (n = 1, 2, 3, 5 and 10), and X is the calcination temperature for Ir/SiO_2. As a control experiment, FeO_x ALD was also performed on the blank SiO_2 support using the same ALD parameters (denoted as nFe/SiO_2), in order to examine the selective deposition of FeO_x on Ir NPs.

2.2. Characterization. The metal contents of the resulting nFe/Ir/SiO_2-X and nFe/SiO_2 catalysts were determined by ICP-AES by dissolving these samples into the hot aqua regia. X-ray diffraction (XRD) patterns of these samples were collected on a Rigaku/Max-3A X-ray diffractometer with Cu Kα radiation (λ = 1.54178 Å), where the operation voltage and current were maintained at 40 kV and 200 mA, respectively. The measurements of aberration-corrected high-angle annular dark-field scanning transmission electron microscopy (HAADF-STEM) were performed on a JEM-ARM200F instrument operated at 200 kV (University of Science and Technology of China) to characterize the morphology of catalysts. Meanwhile, energy-dispersive X-ray (EDX) spectroscopy was also collected on the same equipment.

DRIFTS of CO chemisorption measurements were performed on a Nicolet iS10 spectrometer equipped with a mercury cadmium telluride (MCT) detector and a low-temperature reaction cell (Praying Mantis Harrick). Before each measurement, a sample was calcined in 10 vol % O_2 in He for 1 h at 200 °C and then reduced in 10 vol % H_2 in He for another 2 h at 200 °C. After the sample cooled down to room temperature, a background spectrum was collected. Then, 10 vol % CO in He was carried into the sample cell at a flow rate of 20 mL/min for about 40 min until saturation. Subsequently, the sample was purged with He at a flow rate of 20 mL/min for another 40 min to remove the gas-phase CO or physically adsorbed CO, and then the DRIFT spectra were collected with 256 scans at a resolution of 4 cm^{-1}.

H_2 temperature-programmed reduction (H_2-TPR) was recorded on AutoChem II 2920 equipment (Micromeritics). After loading 50 mg of sample into the U-type quartz tube, the sample was first calcined with 10 vol % O_2 in He at 200 °C for 1 h. Next, the sample was cooled to room temperature or 0 °C, and He was used to purge the reactor for 30 min. Then, the flowing gas was switched to 10 vol % H_2 in He, and the temperature of the catalyst was raised to 700 °C at a ramping rate of 10 °C/min.

2.3. Catalytic Activity Test. The catalytic performances of the Ir catalysts in the PROX and CO oxidation (COOX) reactions were both evaluated in a U-type quartz tube fixed-bed reactor at atmospheric pressure. An amount of 100 mg of Ir/SiO_2 mixed with 1 g of 60−80 mesh quartz chips was used for the reaction test, while the amount of nFe/Ir/SiO_2-X samples was adjusted to keep the same content of Ir. Prior to the reaction test, the catalyst was first oxidized in 10% O_2 in Ar at 200 °C for 1 h and then reduced in 10% H_2 in Ar at 200 °C

DOI: 10.1021/acs.jpcc.9b09066
J. Phys. Chem. C XXXX, XXX, XXX−XXX

for another 2 h. Next, the sample was cooled to room temperature to start the reaction. For the PROX reaction, the gas feed contained 1 vol % CO, 1 vol % O_2, 48 vol % H_2, and Ar balance with a space velocity of 18 000 mL/h/g_{Cat}. For the COOX reaction, the gas feed contained 1 vol % CO, 10 vol % O_2, and Ar balance with a space velocity of 36 000 mL/h/g_{Cat}. The composition at the reactor outlet was analyzed by an online gas chromatograph (Shimadzu GC-2014).

3. RESULTS AND DISCUSSION

3.1. Selective Deposition of FeO_x on Ir NPs. Selective deposition of FeO_x on Ir NPs but not on the silica support (Figure 1a) would allow exploring the properties of the Fe species on Ir NPs without any interference of the ones on the silica support. Such selective deposition was achieved by lowering the deposition temperature to 120 °C, far below the conventional temperatures of 300−350 °C for the FeO_x ALD using ferrocene and O_2;[29,30] therein, the surface reaction between ferrocene and the SiO_2 support was completely prohibited. In addition, variation of the number of ALD cycles would precisely tune the coverage of FeO_x on Ir NPs, thus modulating the interfacial sites between Ir and FeO_x.

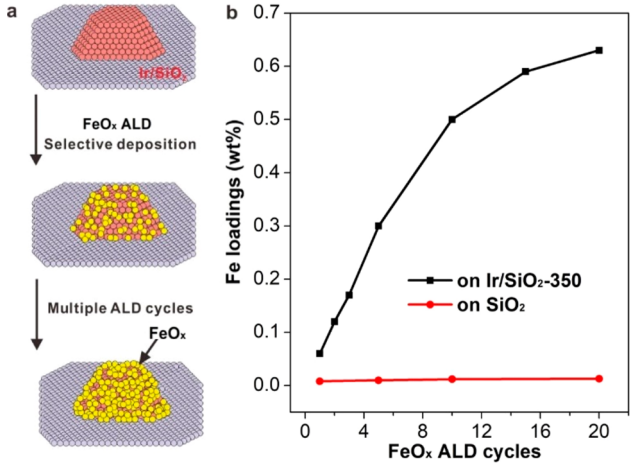

Figure 1. (a) Schematic illustration of selective deposition of FeO_x ALD on Ir/SiO_2 catalysts to tune Ir-FeO_x interfacial sites by varying the number of FeO_x ALD cycles. (b) A plot of the Fe loadings as a function of FeO_x ALD cycles on the Ir/SiO_2-350 catalyst and blank SiO_2 support.

In order to confirm the selective deposition, Ir/SiO_2-350 with an Ir loading of 3.70 wt % was chosen to be a representative catalyst, and different cycles of FeO_x ALD were applied on Ir/SiO_2-350 as well as the blank SiO_2 support. The ICP results of Fe loadings with respect to *n*Fe/Ir/SiO_2-350 catalysts were shown in Figure 1b. In the first five cycles, the Fe loadings increased nearly linearly as a function of ALD cycles, which were 0.06, 0.12, 0.17, and 0.30 wt % in 1Fe/Ir/SiO_2-350, 2Fe/Ir/SiO_2-350, 3Fe/Ir/SiO_2-350, and 5Fe/Ir/SiO_2-350, respectively. Further increasing the number of FeO_x ALD cycles, the increase in Fe loadings became slower, and the Fe loading reached only 0.63 wt % after applying 20 cycles of FeO_x ALD, close to saturation. The slower growth rate of Fe loadings on 10Fe/Ir/SiO_2-350 and 20Fe/Ir/SiO_2-350 indicates that the Ir NPs are gradually covered up. In sharp contrast, after applying 5 cycles and 20 cycles of FeO_x ALD on the bare SiO_2 support, the Fe loadings were nearly negligible, only 0.01 wt %. Thus, the above ICP results clearly demonstrate that FeO_x can be selectively deposited on the Ir NPs in Ir/SiO_2 catalysts but not on the SiO_2 support, in line with our recent work.[27] On the other hand, the absence of growth of FeO_x ALD on oxide surfaces at 120 °C suggests that 20 cycles of FeO_x ALD on Ir NPs reached the nearly full monolayer coverage, which is the maximum FeO_x coverage on Ir NPs. Consequently, the FeO_x coverages of other samples, normalized by the Fe loadings, were about 0.10, 0.19, 0.27, 0.48, 0.79, and 0.95 monolayers, for the 1c, 2c, 3c, 5c, 10c, and 16c of FeO_x-coated Ir/SiO_2-350 samples, respectively. In addition, the Fe loadings of 2Fe/Ir/SiO_2-UC, 2Fe/Ir/SiO_2-250, and 2Fe/Ir/SiO_2-600 were 0.12, 0.15, and 0.11 wt %, respectively, which are all close to that (0.12 wt %) of 2Fe/Ir/SiO_2-350. To note, the Ir loadings in these Ir/SiO_2 catalysts with FeO_x overcoating were all about 3.70 wt %, nearly the same as the uncoated one, due to the low loadings of Fe.

3.2. Morphology. XRD was conducted on Ir/SiO_2 samples with and without FeO_x overcoats. The uncoated Ir/SiO_2 samples calcined at 350 °C or below showed a very weak diffraction peak at 40.5° (Figure 2), assigned to Ir(111) according to PDF card 9008470, indicating ultrasmall Ir particles in these samples. When the sample was calcined at 600 °C, the diffraction peaks at 40.5 and 47.5° became more pronounced, where the latter peak is assigned to Ir(200),[31,32] indicating the growth of Ir particle size with the increase of calcination temperature. XRD was also conducted on 2Fe/Ir/SiO_2-250, 2Fe/Ir/SiO_2-350, and 2Fe/Ir/SiO_2-600 to evaluate the possible aggregation of Ir NPs during FeO_x ALD. It was found that the diffraction peaks in these XRD spectra remained intact after FeO_x ALD, suggesting FeO_x ALD did not affect the size of Ir NPs, in line with previous studies.[27,33−35] In addition, there was no sign of diffraction peaks with respect to the Fe species due to their high dispersion as we found in the system of FeO_x on Pt NPs in our recent work.[27]

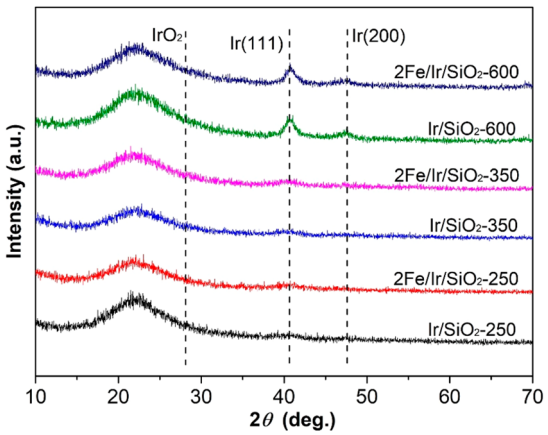

Figure 2. XRD patterns of Ir/SiO_2-*X* and *n*Fe/Ir/SiO_2-*X* catalysts. Prior to XRD measurement, all the catalysts were calcined in 10 vol % O_2 in Ar followed by reduction in 10 vol % H_2 in Ar at 200 °C.

Since FeO_x ALD did not affect the size of Ir NPs, FeO_x-coated Ir/SiO_2 catalysts were selected to perform the STEM measurements to investigate the morphology of Ir NPs. As shown in Figure 3, the size of Ir NPs in 2Fe/Ir/SiO_2-UC, 2Fe/Ir/SiO_2-250, 2Fe/Ir/SiO_2-350, and 2Fe/Ir/SiO_2-600 was 1.5 ± 0.6, 2.0 ± 0.3, 2.1 ± 0.5, and 4.2 ± 0.8 nm, respectively. Higher calcination temperature produces larger Ir particle size, which is consistent with the XRD analysis in Figure 2. In

DOI: 10.1021/acs.jpcc.9b09066
J. Phys. Chem. C XXXX, XXX, XXX−XXX

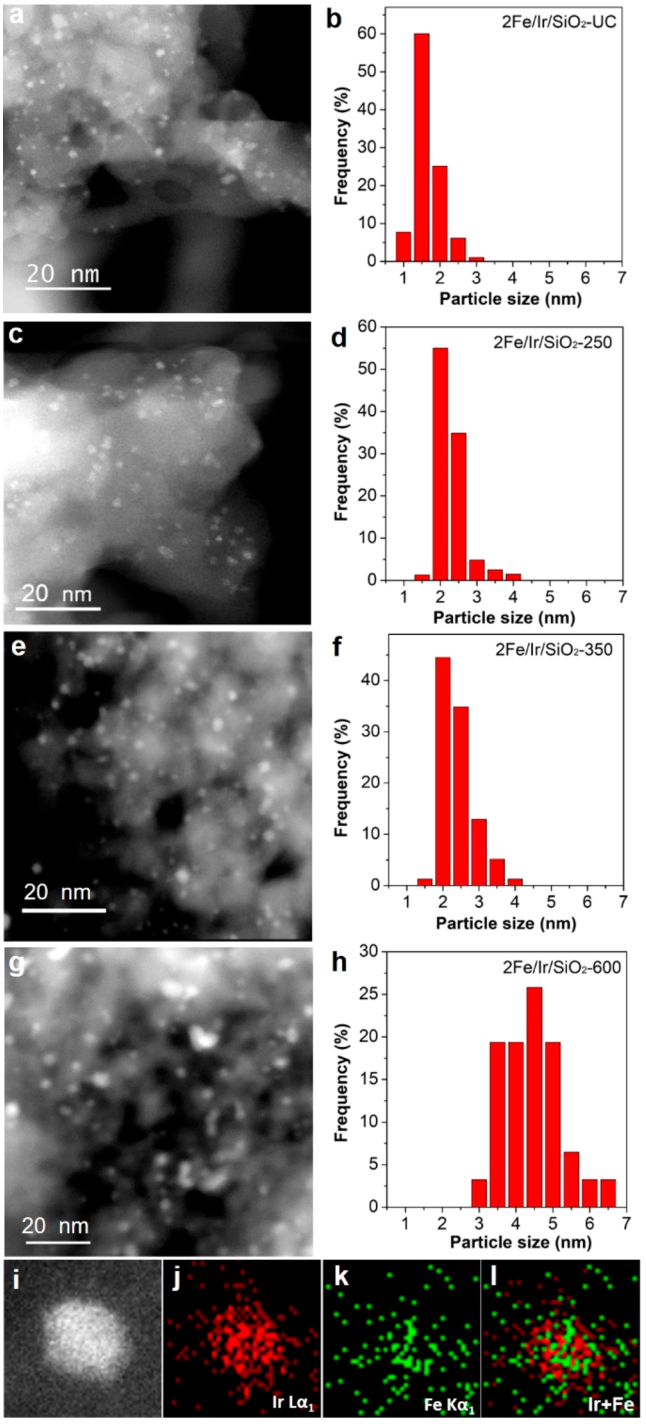

Figure 3. HAADF-STEM images of different Ir−Fe catalysts. (a,b) 2Fe/Ir/SiO_2-UC; (c,d) 2Fe/Ir/SiO_2-250; (e,f) 2Fe/Ir/SiO_2-350; and (g,h) 2Fe/Ir/SiO_2-600. (i) 10Fe/Ir/SiO_2-350 and the corresponding EDX mapping images: (j) Ir Lα1 and (k) Fe Kα1 signals and (l) the reconstructed Ir−Fe composition.

addition, elemental mapping using the energy-dispersive X-ray spectroscopy (EDS) was also carried out to further verify the selective deposition of FeO_x on Ir NPs. In order to achieve a better contrast of the Fe species in the samples, 10Fe/Ir/SiO_2-350 with a high Fe content was selected for the EDS elemental mapping. As shown in Figure 3i−l, the Fe signal overlapped with the Ir signal, again unambiguously confirming the selective deposition of FeO_x on Ir NPs, in line with the ICP results (Figure 1b).

3.3. In Situ DRIFTS CO Chemisorption. In situ DRIFTS CO chemisorption measurements were performed to study the gradual FeO_x overcoating on the Ir/SiO_2-350 catalyst with an increase of ALD cycles. As shown in Figure 4, the sample

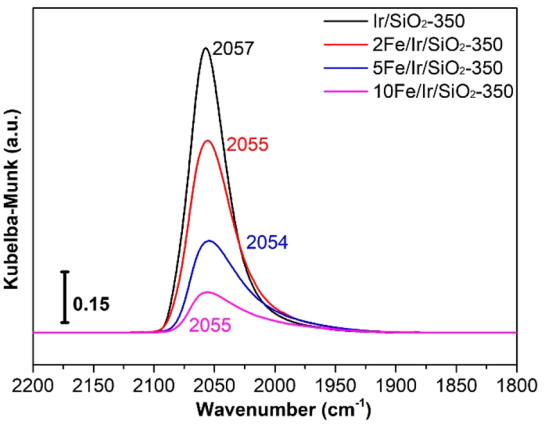

Figure 4. In situ DRIFTS spectra of CO chemisorption on *n*Fe/Ir/SiO_2-350 catalysts.

without an FeO_x overcoat showed a strong peak at 2057 cm^{-1}, corresponding to the linear CO chemisorbed on Ir NPs.[32] After two cycles of FeO_x overcoating, the intensity of the CO chemisorption peak decreased remarkably, along with a small red shift to 2054 cm^{-1}, indicating the Ir NPs are partially covered by the FeO_x overcoat, indicating the formation of Ir−FeO_x interfaces. The intensity of the CO chemisorption peak continually decreased with increasing ALD cycles, implying that the Ir particle surfaces were gradually covered up. The DRIFTS CO spectra of the FeO_x-coated Ir samples were identical to the uncoated one in shape, which might suggest a rather uniform coating of Ir particles. On the other hand, DRIFTS spectra in Kubelka−Munk units can also provide a good estimation of FeO_x coverage on Ir NPs since the amount of chemisorbed CO is close to a linear relationship with the IR peak intensity.[36,37] Quantification of the CO peak intensities in Figure 4 revealed that the FeO_x coverages were about 0.21, 0.60, and 0.80 monolayers for the 2c, 5c, and 10c of FeO_x-coated samples, respectively, which agree very well with the one determined by the Fe loadings. In brief, the DRIFTS CO chemisorption results clearly describe the precise tailoring of the Ir−FeO_x interfacial sites by varying the number of FeO_x ALD cycles.

3.4. H_2-TPR. H_2-TPR was also carried out on Ir/SiO_2-350 and *n*Fe/Ir/SiO_2-350 (n = 2, 5, 10) to investigate the reduction properties of Fe species. As a control experiment, H_2-TPR was also performed on a Fe/SiO_2 sample, which was synthesized by FeO_x ALD at 290 °C for 10 cycles. It was found that there were several broad reduction peaks between 250 and 650 °C, with the main peak located at 567 °C (Figure 5), corresponding to the complete reduction of Fe^{3+} species on SiO_2 to metallic Fe.[38] The major reduction peak of the Ir/SiO_2-350 catalyst locates at about 92 °C with a H_2 consumption of 156 μmol/g_{cat}, which is assigned to the reduction of Ir oxide to metallic Ir. The remaining three weaker features at ~210, 335, and 465 °C might be attributed to the reduction of Ir species at the interfaces between Ir and SiO_2 support.[21,39] When two cycles of FeO_x ALD were applied

DOI: 10.1021/acs.jpcc.9b09066
J. Phys. Chem. C XXXX, XXX, XXX−XXX

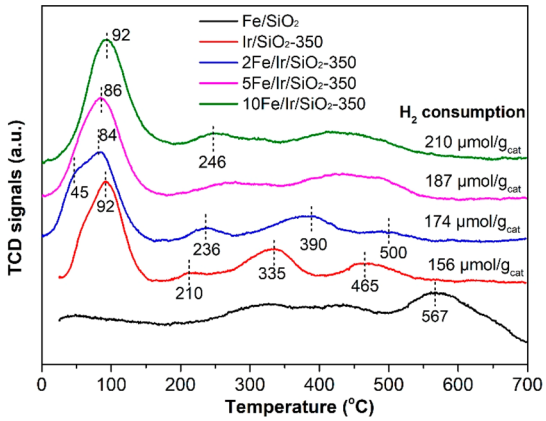

Figure 5. H_2-TPR profiles of nFe/Ir/SiO_2-350 and Fe/SiO_2 samples. The amount of H_2 consumption for the strong reduction peak between 0 and 150 °C is indicated for the nFe/Ir/SiO_2-350 samples.

onto Ir/SiO_2-350, the main reduction peak shifted to a lower temperature of 84 °C, along with a shoulder at around 45 °C. The H_2 consumption of this main peak increased to 174 μmol/g_{cat}. This result infers that the reduction of FeO_x species from Fe^{3+} to Fe^{2+} probably appeared at around 45 °C, in line with our observation of the reduction of the Fe species on Pt NPs from Fe^{3+} to Fe^{2+} at room temperature.[27] The remaining three weaker features remained 2Fe/Ir/SiO_2-350 but shifted slightly to higher temperatures of ~236, 390, and 500 °C, respectively, an indication of the strong interaction between Ir and FeO_x.

Increasing the number of FeO_x ALD cycles, the main reduction peak shifted to higher temperatures of 86 and 92 °C with an increased H_2 consumption also increased to 187 and 210 μmol/g_{cat}, on 5Fe/Ir/SiO_2-350 and 10Fe/Ir/SiO_2-350, respectively. Such a shift of reduction peak with the increase of FeO_x ALD cycles might be attributed to the decreased reducibility with the increase in the FeO_x size, again in line with the case of FeO_x on Pt NPs.[27]

3.5. Catalytic Performance. Here, the representative catalysts of nFe/Ir/SiO_2-350 with different cycles of FeO_x ALD overcoating (n = 0, 1, 2, 3, 5, and 10) were first selected to investigate the catalytic performance in the COOX and PROX reaction as a function of the number of FeO_x ALD cycles. In the absence of H_2, the catalytic activity in the COOX reaction was rather low for all the catalysts (Figure 6a). The uncoated Ir/SiO_2-350 sample showed negligible CO conversion at below 120 °C. After FeO_x overcoating, the CO conversions on all these samples at below 120 °C were still only ~2 to 10%. Complete CO conversion was achieved at literally the same temperature of 180 °C on all these samples. It appears that the Ir−FeO_x interfacial sites formed in nFe/Ir/SiO_2-350 have limited improvements on the CO oxidation activity in the absence of H_2, in line with the literature in regard to the low activity of Ir−Fe catalysts in CO oxidation.[38,40]

In sharp contrast to the catalytic behaviors in COOX, FeO_x exhibited a remarkable activity enhancement in the PROX reaction. As shown in Figure 6b, the uncoated Ir/SiO_2-350 catalyst showed a low CO conversion of less than 10% at below 120 °C, and the CO conversion only reached 86% at 200 °C, consistent with the literature.[38] However, after one cycle of FeO_x overcoating, the catalytic performance was improved dramatically by achieving 100% CO conversion in the temperature range of 120−160 °C. When two cycles of FeO_x overcoating were applied on Ir/SiO_2-350, the CO

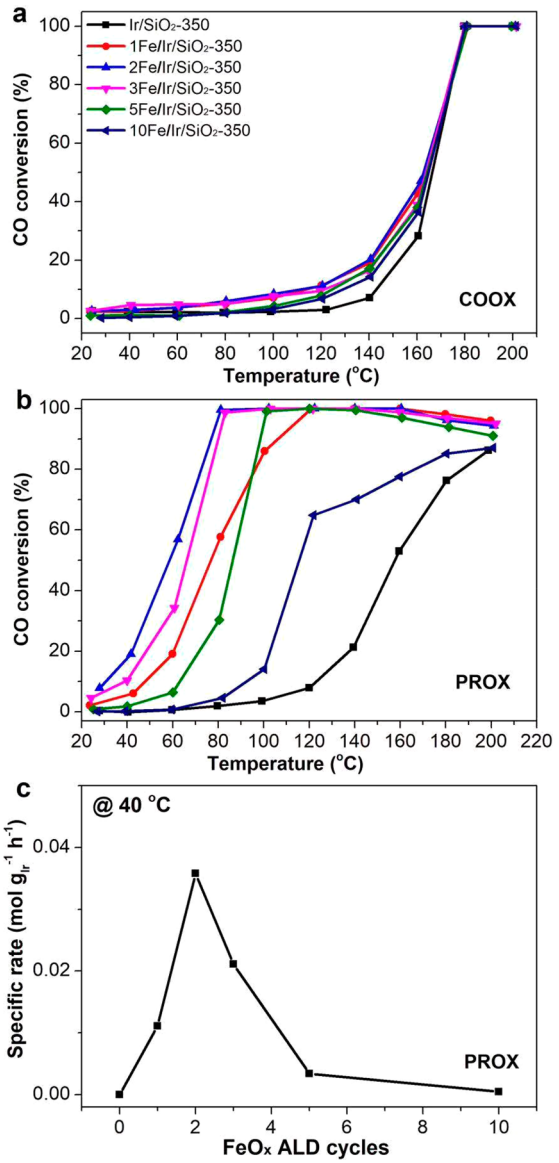

Figure 6. Catalytic performance of nFe/Ir/SiO_2-350 catalysts in the COOX and PROX reaction. (a) COOX. Reaction condition: 1 vol % CO; 10 vol % O_2; Ar balance. Weight hourly space velocity: 36 000 mL h^{-1} g_{cat}^{-1}. (b) PROX. Reaction condition: 1 vol % CO; 1 vol % O_2; 48 vol % H_2; Ar balance. Weight hourly space velocity: 18 000 mL h^{-1} g_{cat}^{-1}. (c) A plot of specific rates in the PROX reaction at 40 °C as a function of FeO_x ALD cycles.

conversion was about 20% at 40 °C and rapidly increased to 100% at 80 °C, yielding a temperature window of 80−160 °C for complete CO conversion.

The catalytic performance of 3Fe/Ir/SiO_2-350 was very similar to 2Fe/Ir/SiO_2-350. While further increasing the number of FeO_x ALD cycles, the activity decreased considerably. On 10Fe/Ir/SiO_2-350, the maximum CO conversion was only ~87% at 200 °C. Figure 6c plots the specific rates of these nFe/Ir/SiO_2-350 catalysts in the PROX reaction at 40 °C as a function of FeO_x ALD cycles. It was found that the specific rates were in a volcano-like shape as a function of ALD cycles, with a maximum rate of 0.036 mol g_{Ir}^{-1} h^{-1} achieved on 2Fe/Ir/SiO_2-350. Taking the FeO_x coverages on Ir NPs as determined by ICP-AES (Figure 1) and the DRIFTS measurements (Figure 4) into account, these

DOI: 10.1021/acs.jpcc.9b09066
J. Phys. Chem. C XXXX, XXX, XXX−XXX

results suggest that the Ir−FeO_x interfacial sites are the active sites in the PROX reaction, and the number of these interfacial sites is varied in a volcano-like trend as a function of ALD cycles.[33] On the other hand, the higher reducibility of FeO_x species in 2Fe/Ir/SiO_2-350 than those in 5Fe/Ir/SiO_2-350 and 10Fe/Ir/SiO_2-350 (Figure 5) might also contribute to the high activity of 2Fe/Ir/SiO_2-350 considerably.

The presence of H_2 showed a dramatic activity promotion on the FeO_x-coated Ir/SiO_2-350 samples but not on the uncoated one (Figure 6b). Such an activity promotion by H_2 on the Ir/$Fe(OH)_x$ catalyst was also reported by Zhang et al.[40] They attributed such a promotion to the formation of hydroxyl groups on the FeO_x support. Tanaka et al. also suggested that CO reacts with surface OH instead of oxygen to form a HCOO intermediate on the FeO_x/Pt/TiO_2 catalyst in the PROX reaction, thus largely improving the CO oxidation activity.[41] Recently, we also found that in the PROX reaction the Fe species in the ALD-FeO_x-decorated Pt catalyst was atomically dispersed iron hydroxide, $Fe_1(OH)_3$.[27] Therefore, the remarkable H_2 promotion of CO oxidation activity on the FeO_x-coated Ir/SiO_2-350 samples can be attributed to the formation of rich hydroxyl groups on the FeO_x overcoat.

3.6. Particle Size Effect on the Catalytic Performance.

To investigate the Ir particle size effect on the catalytic performance, two cycles of FeO_x ALD were also performed on other Ir/SiO_2 samples, where the size of Ir NPs was tuned from 1.5 ± 0.6 to 4.2 ± 0.8 nm by varying the calcination temperature (Figures 2 and 3). As shown in Figure 7a, the activity in COOX showed a strong Ir particle size dependence, and the smaller the Ir particle size, the higher the activity. The 2Fe/Ir/SiO_2-600 sample with a particle size of 4.2 ± 0.8 nm showed a poor activity by achieving 20% CO conversion even at 160 °C, while the 2Fe/Ir/SiO_2-UC sample, with the smallest Ir particle size of 1.5 ± 0.6 nm, showed a remarkably high activity in CO oxidation, by achieving ∼20% CO conversion even at 28 °C and complete CO conversion at 120 °C. The increased amount of Ir−FeO_x interfacial sites and the varied CO adsorption strength on the smaller size of Ir NPs as observed on other Pt-group metals[42−45] might play a major role.

In the PROX reaction, a similar trend of particle size on the activity was observed (Figure 7b). On the 2Fe/Ir/SiO_2-600 sample, the maximum CO conversion was only about 90% at 120 °C, which kept nearly constant at the temperatures between 120 and 160 °C. On 2Fe/Ir/SiO_2-250, the complete CO conversion was achieved at between 80 and 180 °C, slightly broader than the complete CO conversion temperature window (80−160 °C) achieved on 2Fe/Ir/SiO_2-350. Further decreasing the particle size to 1.5 ± 0.6 nm, 2Fe/Ir/SiO_2-UC showed an even broader complete CO conversion temperature window of 60−180 °C, which is the broadest temperature window for complete CO conversion in the PROX reaction over Ir-based catalysts reported and also among the broadest ones for all catalysts reported in the literature (Table 1). The observation of higher activity on the smaller Ir particle size sample in the CO oxidation and PROX reaction here also agrees excellently with the literature on the Ir/$Fe(OH)_x$ catalyst in the PROX reaction.[21] Based on the achievement of the low-temperature window of 20−60 °C for the complete CO conversion over subnanometer Ir clusters,[21] we speculate that downsizing the Ir particle size to the subnanometer range along with our strategy of FeO_x coating might allow the

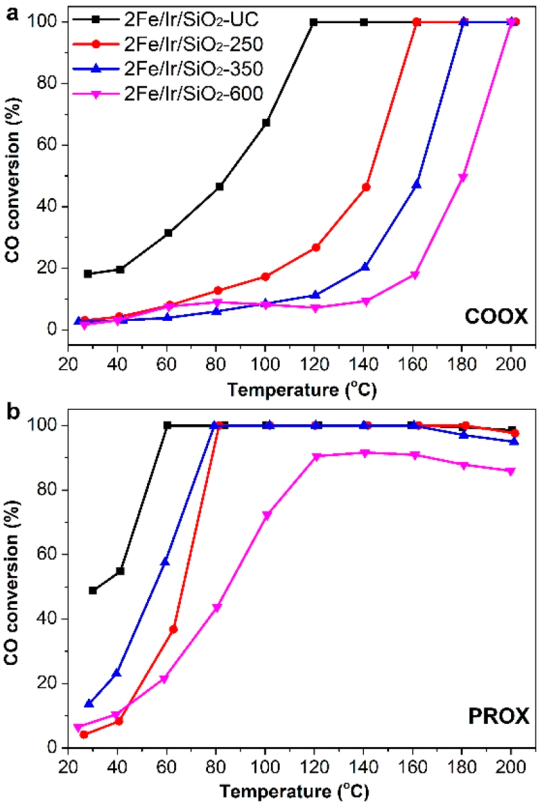

Figure 7. Size-dependent catalytic activity of the 2Fe/Ir/SiO_2-*X* catalyst in the COOX and PROX reaction. (a) COOX. Reaction condition: 1 vol % CO; 10 vol % O_2; Ar balance. Weight hourly space velocity: 36 000 mL h^{-1} g_{cat}^{-1}. (b) PROX. Reaction condition: 1 vol % CO; 1 vol % O_2; 48 vol % H_2; Ar balance. Weight hourly space velocity: 18 000 mL h^{-1} g_{cat}^{-1}.

achievement of broadening the low onset temperature to 20 °C.

The stability of the 2Fe/Ir/SiO_2-UC catalyst in the PROX reaction was also evaluated at the operation temperature of 80 °C for PEMFCs. We found that the catalyst was very stable by preserving CO conversion of 100% and selectivity of 50% for at least 20 h (Figure 8a). We further examined this catalyst at a more severe condition of 200 °C and found a similar result by preserving CO conversion at 95% in 24 h (Figure 8b). These results suggest that the Ir−FeO_x interfacial sites generated by ALD are stable under the PROX reaction conditions.

4. CONCLUSION

In summary, we have demonstrated that selective deposition of the FeO_x overcoat onto SiO_2-supported Ir NPs using ALD allows precisely tailoring Ir−FeO_x interfacial sites for optimized catalytic activity. ICP-AES and EDS elemental mapping confirmed the selective deposition. We found that the deposition of FeO_x on Ir NPs could largely enhance the CO oxidation activity in the PROX reaction by showing a volcano trend as a function of the numbers of FeO_x ALD cycles; therein, the 2Fe/Ir/SiO_2-UC catalyst with an Ir particle size of 1.5 ± 0.6 nm showed a temperature range of 60−180 °C for complete CO oxidation in the PROX reaction, a broadest temperature window over Ir-based catalysts reported in the literature so far. These results strongly indicate that the Ir−FeO_x interfacial sites are the active sites. Interestingly, the activity promotion by FeO_x in the PROX reaction was found

DOI: 10.1021/acs.jpcc.9b09066
J. Phys. Chem. C XXXX, XXX, XXX−XXX

Table 1. Comparison of the Catalytic Performances of Our 2Fe/Ir/SiO_2-UC Catalyst with the Representative Noble Metal Catalysts Reported in the Literature

catalysts	noble metal loadings (wt %)	transition metal loading (wt %)	composition of feed gas (%) CO	O_2	H_2	space velocity (mL $h^{-1}g_{cat}^{-1}$)	maximal CO conversion (%)	temperature window for the maximal CO conversion (°C)	notes
2Fe/Ir/SiO_2-UC	3.7	0.12	1	1	48	18000	100	60−180	this work
Ir/Fe(OH)$_x$	2.4	NA[a]	1	1	40	18000	100	20−60	ref 21
Ir-Fe/SiO_2	3	4.4	2	1	10	40000	85	100−120	ref 38
$IrFe_5/Al_2O_3$	1	5	2	1	40	40000	68	100	ref 39
Ir in CeO_2	1.6	NA	2	1	40	40000	77	140	ref 46
Ir/CeO_2	2	NA	2	1	70	60000	60	90	ref 47
1cFe−Pt/SiO_2	3.6	0.1	1	0.5	48	36000	100	−75−107	ref 27
Pt−Fe/SiO_2	4	0.5	1	0.5	98.5	36000	100	27−47	ref 19
Pt−Fe/Al_2O_3	0.7	0.23	1	1	50	20000	100	25−55	ref 48
Pt−Fe/zeolite	4	2	1	0.5	98.5	120000	100	80−200	ref 18
Au/Fe_2O_3	4.4	NA	1	1	40	18750	100	20−40	ref 17
Au_1/CeO_2 (single atom)	0.05	NA	1	1	40	25000	100	70−120	ref 12

[a]NA: Not applicable.

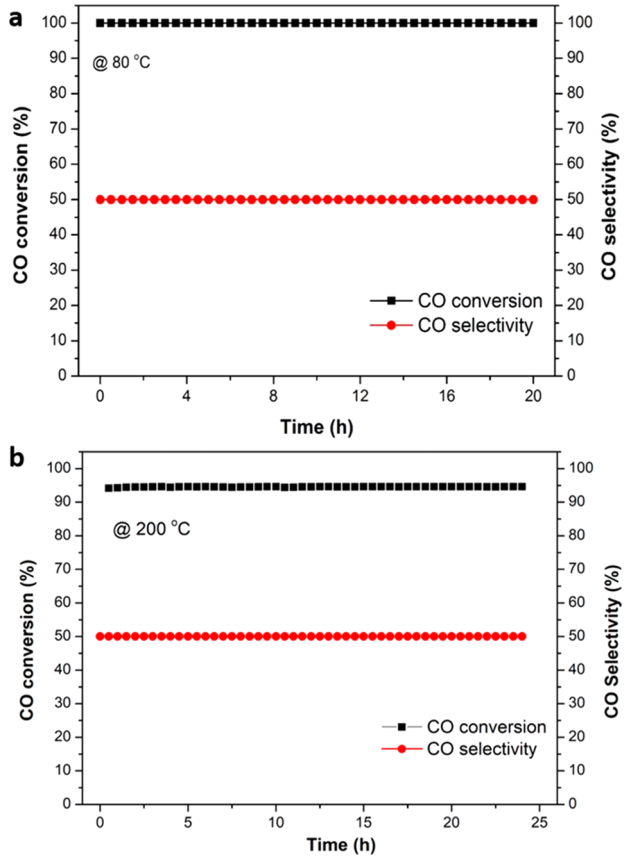

Figure 8. Stability of the 2Fe/Ir/SiO_2-UC catalyst in the PROX reaction at 80 °C (a) and 200 °C (b). Reaction conditions: 1 vol % CO; 1 vol % O_2; 48 vol % H_2; Ar balance; and weight hourly space velocity was 18000 mL h^{-1} g_{cat}^{-1} for (a) and 36000 mL h^{-1} g_{cat}^{-1} for (b).

to be much greater than that in the COOX reaction in the absence of H_2. This result infers that hydroxyls are likely formed on the FeO_x overcoat under the PROX reaction conditions.

AUTHOR INFORMATION

Corresponding Author

*E-mail: junling@ustc.edu.cn.

ORCID

Junjie Li: 0000-0001-5845-7204

Junling Lu: 0000-0002-2607-6869

Notes

The authors declare no competing financial interest.

ACKNOWLEDGMENTS

This work was supported by the National Natural Science Foundation of China (Grant number 21673215), the Fundamental Research Funds for the Central Universities, China (WK2060030029, WK6030000015), Users with Excellence Program of Hefei Science Center CAS (2019HSC-UE016), and the Max-Planck Partner Group.

REFERENCES

(1) Liu, K.; Wang, A.; Zhang, T. Recent advances in preferential oxidation of CO reaction over platinum group metal catalysts. *ACS Catal.* **2012**, *2*, 1165−1178.

(2) Kotobuki, M.; Watanabe, A.; Uchida, H.; Yamashita, H.; Watanabe, M. Reaction mechanism of preferential oxidation of carbon monoxide on Pt, Fe, and Pt−Fe/mordenite catalysts. *J. Catal.* **2005**, *236*, 262−269.

(3) Haryanto, A.; Fernando, S.; Murali, N.; Adhikari, S. Current status of hydrogen production techniques by steam reforming of ethanol: A review. *Energy Fuels* **2005**, *19*, 2098−2106.

(4) Park, E. D.; Lee, D.; Lee, H. C. Recent progress in selective CO removal in a H_2-rich stream. *Catal. Today* **2009**, *139*, 280−290.

(5) Hultquist, G. Hydrogen evolution in corrosion of copper in pure water. *Corros. Sci.* **1986**, *26*, 173−177.

(6) Zhang, R.; Ludviksson, A.; Campbell, C. T. The chemisorption of H_2O and O_2 on Cu films on ZnO (0001)-O. *Surf. Sci.* **1993**, *289*, 1−9.

(7) Quinet, E.; Morfin, F.; Diehl, F.; Avenier, P.; Caps, V.; Rousset, J. Hydrogen effect on the preferential oxidation of carbon monoxide over alumina-supported gold nanoparticles. *Appl. Catal., B* **2008**, *80*, 195−201.

(8) Bion, N.; Epron, F.; Moreno, M.; Marino, F.; Duprez, D. Preferential oxidation of carbon monoxide in the presence of

DOI: 10.1021/acs.jpcc.9b09066
J. Phys. Chem. C XXXX, XXX, XXX−XXX

hydrogen (PROX) over noble metals and transition metal oxides: Advantages and drawbacks. *Top. Catal.* **2008**, *51*, 76−88.
(9) Marbán, G.; Fuertes, A. B. Highly active and selective CuO_x/CeO_2 catalyst prepared by a single-step citrate method for preferential oxidation of carbon monoxide. *Appl. Catal., B* **2005**, *57*, 43−53.
(10) Manzoli, M.; Di Monte, R.; Boccuzzi, F.; Coluccia, S.; Kašpar, J. CO oxidation over CuOx-CeO_2-ZrO_2 catalysts: Transient behaviour and role of copper clusters in contact with ceria. *Appl. Catal., B* **2005**, *61*, 192−205.
(11) Grisel, R.; Nieuwenhuys, B. Selective oxidation of CO, over supported Au catalysts. *J. Catal.* **2001**, *199*, 48−59.
(12) Qiao, B.; Liu, J.; Wang, Y.-G.; Lin, Q.; Liu, X.; Wang, A.; Li, J.; Zhang, T.; Liu, J. Highly efficient catalysis of preferential oxidation of CO in H_2-rich stream by gold single-atom catalysts. *ACS Catal.* **2015**, *5*, 6249−6254.
(13) Haruta, M. Size-and support-dependency in the catalysis of gold. *Catal. Today* **1997**, *36*, 153−166.
(14) Han, Y.-F.; Kinne, M.; Behm, R. Selective oxidation of CO on Ru/γ-Al_2O_3 in methanol reformate at low temperatures. *Appl. Catal., B* **2004**, *52*, 123−134.
(15) Okumura, M.; Masuyama, N.; Konishi, E.; Ichikawa, S.; Akita, T. CO oxidation below room temperature over Ir/TiO_2 catalyst prepared by deposition precipitation method. *J. Catal.* **2002**, *208*, 485−489.
(16) Lin, J.; Wang, X.; Zhang, T. Recent progress in CO oxidation over Pt-group-metal catalysts at low temperatures. *Chin. J. Catal.* **2016**, *37*, 1805−1813.
(17) Qiao, B.; Wang, A.; Li, L.; Lin, Q.; Wei, H.; Liu, J.; Zhang, T. Ferric oxide-supported Pt subnano clusters for preferential oxidation of CO in H_2-rich gas at room temperature. *ACS Catal.* **2014**, *4*, 2113−2117.
(18) Watanabe, M.; Uchida, H.; Ohkubo, K.; Igarashi, H. Hydrogen purification for fuel cells: selective oxidation of carbon monoxide on Pt−Fe/zeolite catalysts. *Appl. Catal., B* **2003**, *46*, 595−600.
(19) Fu, Q.; Li, W.-X.; Yao, Y.; Liu, H.; Su, H.-Y.; Ma, D.; Gu, X.-K.; Chen, L.; Wang, Z.; Zhang, H.; et al. Interface-confined ferrous centers for catalytic oxidation. *Science* **2010**, *328*, 1141−1144.
(20) Zhang, W.; Huang, Y.; Wang, J.; Liu, K.; Wang, X.; Wang, A.; Zhang, T. $IrFeO_x$/SiO_2—A highly active catalyst for preferential CO oxidation in H_2. *Int. J. Hydrogen Energy* **2010**, *35*, 3065−3071.
(21) Lin, J.; Qiao, B.; Liu, J.; Huang, Y.; Wang, A.; Li, L.; Zhang, W.; Allard, L. F.; Wang, X.; Zhang, T. Design of a highly active Ir/$Fe(OH)_x$ catalyst: versatile application of Pt-group metals for the preferential oxidation of carbon monoxide. *Angew. Chem.* **2012**, *124*, 2974−2978.
(22) George, S. M. Atomic layer deposition: an overview. *Chem. Rev.* **2010**, *110*, 111−31.
(23) Suntola, T.; Antson, J. US Patent 4058430, 1977.
(24) Hoivik, N. D.; Elam, J. W.; Linderman, R. J.; Bright, V. M.; George, S. M.; Lee, Y. Atomic layer deposited protective coatings for micro-electromechanical systems. *Sens. Actuators, A* **2003**, *103*, 100−108.
(25) Groner, M.; George, S.; McLean, R.; Carcia, P. Gas diffusion barriers on polymers using Al_2O_3 atomic layer deposition. *Appl. Phys. Lett.* **2006**, *88*, 051907.
(26) Puurunen, R. L. Surface chemistry of atomic layer deposition: A case study for the trimethylaluminum/water process. *J. Appl. Phys.* **2005**, *97*, 121301.
(27) Cao, L.; Liu, W.; Luo, Q.; Yin, R.; Wang, B.; Weissenrieder, J.; Soldemo, M.; Yan, H.; Lin, Y.; Sun, Z.; et al. Atomically dispersed iron hydroxide anchored on Pt for preferential oxidation of CO in H_2. *Nature* **2019**, *565*, 631.
(28) Haneda, M.; Kudo, H.; Nagao, Y.; Fujitani, T.; Hamada, H. Enhanced activity of Ba-doped Ir/SiO_2 catalyst for NO reduction with CO in the presence of O_2 and SO_2. *Catal. Commun.* **2006**, *7*, 423−426.
(29) Rooth, M. r.; Johansson, A.; Kukli, K.; Aarik, J.; Boman, M.; Hårsta, A. Atomic layer deposition of iron oxide thin films and nanotubes using ferrocene and oxygen as precursors. *Chem. Vap. Deposition* **2008**, *14*, 67−70.
(30) Scheffe, J. R.; Francés, A.; King, D. M.; Liang, X.; Branch, B. A.; Cavanagh, A. S.; George, S. M.; Weimer, A. W. Atomic layer deposition of iron (III) oxide on zirconia nanoparticles in a fluidized bed reactor using ferrocene and oxygen. *Thin Solid Films* **2009**, *517*, 1874−1879.
(31) Haneda, M.; Kintaichi, Y.; Nakamura, I.; Sasaki, M.; Fujitani, T.; Hamada, H. Promotional effect of SO_2 on the activity of Ir/SiO_2 for NO reduction with CO under oxygen-rich conditions. *J. Catal.* **2005**, *229*, 197−205.
(32) Haneda, M.; Fujitani, T.; Hamada, H. Effect of iridium dispersion on the catalytic activity of Ir/SiO_2 for the selective reduction of NO with CO in the presence of O_2 and SO_2. *J. Mol. Catal. A: Chem.* **2006**, *256*, 143−148.
(33) Wang, C.; Wang, H.; Yao, Q.; Yan, H.; Li, J.; Lu, J. Precisely applying TiO_2 overcoat on supported Au catalysts using atomic layer deposition for understanding the reaction mechanism and improved activity in CO oxidation. *J. Phys. Chem. C* **2016**, *120*, 478−486.
(34) Yi, H.; Du, H.; Hu, Y.; Yan, H.; Jiang, H.-L.; Lu, J. Precisely controlled porous alumina overcoating on Pd catalyst by atomic layer deposition: Enhanced selectivity and durability in hydrogenation of 1, 3-butadiene. *ACS Catal.* **2015**, *5*, 2735−2739.
(35) Yao, Q.; Wang, C.; Wang, H.; Yan, H.; Lu, J. Revisiting the Au particle size effect on TiO_2-coated Au/TiO_2 catalysts in CO oxidation reaction. *J. Phys. Chem. C* **2016**, *120*, 9174−9183.
(36) Schubert, M.; Kahlich, M.; Gasteiger, H.; Behm, R. Correlation between CO surface coverage and selectivity/kinetics for the preferential CO oxidation over Pt/γ-Al_2O_3 and Au/α-Fe_2O_3: an in-situ DRIFTS study. *J. Power Sources* **1999**, *84*, 175−182.
(37) Eckle, S.; Augustin, M.; Anfang, H.-G.; Behm, R. J. Influence of the catalyst loading on the activity and the CO selectivity of supported Ru catalysts in the selective methanation of CO in CO_2 containing feed gases. *Catal. Today* **2012**, *181*, 40−51.
(38) Liu, K.; Wang, A.; Zhang, W.; Wang, J.; Huang, Y.; Shen, J.; Zhang, T. Quasi in situ ^{57}Fe Mössbauer spectroscopic study: Quantitative correlation between Fe^{2+} and H_2 concentration for PROX over Ir−Fe/SiO_2 catalyst. *J. Phys. Chem. C* **2010**, *114*, 8533−8541.
(39) Zhang, W.; Wang, A.; Li, L.; Wang, X.; Zhang, T. Design of a novel bifunctional catalyst IrFe/Al_2O_3 for preferential CO oxidation. *Catal. Today* **2008**, *131*, 457−463.
(40) Lin, J.; Qiao, B.; Li, L.; Guan, H.; Ruan, C.; Wang, A.; Zhang, W.; Wang, X.; Zhang, T. Remarkable effects of hydroxyl species on low-temperature CO (preferential) oxidation over Ir/$Fe(OH)_x$ catalyst. *J. Catal.* **2014**, *319*, 142−149.
(41) Tanaka, K.-I.; Shou, M.; He, H.; Shi, X.; Zhang, X. Dynamic characterization of the intermediates for low-temperature PROX reaction of CO in H_2 oxidation of CO with OH via HCOO intermediate. *J. Phys. Chem. C* **2009**, *113*, 12427−12433.
(42) Liu, L.; Corma, A. Metal catalysts for heterogeneous catalysis: from single atoms to nanoclusters and nanoparticles. *Chem. Rev.* **2018**, *118*, 4981−5079.
(43) Qiao, B.; Wang, A.; Yang, X.; Allard, L. F.; Jiang, Z.; Cui, Y.; Liu, J.; Li, J.; Zhang, T. Single-atom catalysis of CO oxidation using Pt_1/FeO_x. *Nat. Chem.* **2011**, *3*, 634.
(44) Flores-Camacho, J. M.; Fischer-Wolfarth, J.-H.; Peter, M.; Campbell, C. T.; Schauermann, S.; Freund, H.-J. Adsorption energetics of CO on supported Pd nanoparticles as a function of particle size by single crystal microcalorimetry. *Phys. Chem. Chem. Phys.* **2011**, *13*, 16800−16810.
(45) Ligthart, D. M.; van Santen, R. A.; Hensen, E. J. Supported rhodium oxide nanoparticles as highly active CO oxidation catalysts. *Angew. Chem., Int. Ed.* **2011**, *50*, 5306−5310.
(46) Huang, Y.; Wang, A.; Li, L.; Wang, X.; Su, D.; Zhang, T. Ir-in-ceria": A highly selective catalyst for preferential CO oxidation. *J. Catal.* **2008**, *255*, 144−152.

DOI: 10.1021/acs.jpcc.9b09066
J. Phys. Chem. C XXXX, XXX, XXX−XXX

(47) Mariño, F.; Descorme, C.; Duprez, D. Noble metal catalysts for the preferential oxidation of carbon monoxide in the presence of hydrogen (PROX). *Appl. Catal., B* **2004**, *54*, 59−66.
(48) Zhang, H.; Liu, X.; Zhang, N.; Zheng, J.; Zheng, Y.; Li, Y.; Zhong, C.-J.; Chen, B. H. Construction of ultrafine and stable PtFe nano-alloy with ultra-low Pt loading for complete removal of CO in PROX at room temperature. *Appl. Catal., B* **2016**, *180*, 237−245.

DOI: 10.1021/acs.jpcc.9b09066
J. Phys. Chem. C XXXX, XXX, XXX−XXX